RSC Advances

PAPER

View Article Online
View Journal | View Issue

Cite this: *RSC Adv.*, 2019, **9**, 6064

β-Ga_2O_3 nanorod arrays with high light-to-electron conversion for solar-blind deep ultraviolet photodetection

Shunli Wang,†[a] Kai Chen,†[a] Hailin Zhao,[a] Chenran He,[a] Chao Wu,[a] Daoyou Guo,*[a] Nie Zhao,[c] Goran Ungar,[ad] Jingqin Shen,[a] Xulong Chu,[be] Peigang Li*[b] and Weihua Tang[b]

Vertically aligned nanorod arrays (NRAs), with effective optical coupling with the incident light and rapid electron transport for photogenerated carriers, have attracted much interest for photoelectric devices. Herein, the monoclinic β-Ga_2O_3 NRAs with an average diameter/length of 500 nm/1.287 μm were prepared by the hydrothermal and post-annealing method. Then a circular Ti/Au electrode was patterned on β-Ga_2O_3 NRAs to fabricate solar-blind deep ultraviolet photodetectors. At zero bias, the device shows a photoresponsivity (R_λ) of 10.80 mA W^{-1} and a photo response time of 0.38 s under 254 nm light irradiation with a light intensity of 1.2 mW cm^{-2}, exhibiting a self-powered characteristic. This study presents a promising candidate for use in solar-blind deep ultraviolet photodetection with zero power consumption.

Received 18th December 2018
Accepted 23rd January 2019

DOI: 10.1039/c8ra10371b

rsc.li/rsc-advances

1. Introduction

Solar-blind ultraviolet (UV) photodetectors (PDs) are useful as an answer to the technical challenge of operating at wavelengths less than 290 nm, while exposed to a large background radiation of sunlight. With the continuous improvement of device integration, environment complexity, and interference technology, solar-blind ultraviolet region photodetectors can effectively reduce false alarm rates in early-warning, searching, and tracking systems, to improve the accuracy and versatility of detection systems in various situations.[1–5] Up to now, a number of wide bandgap semiconductors have been investigated to design solar-blind photodetectors, such as AlGaN,[6] ZnMgO,[7] β-Ga_2O_3,[8] *etc*. AlGaN-based photodetectors present more excellent performance than the other wide bandgap semiconductors devices. However, with increasing Al composition for solar-blind detection, the performance of AlGaN photodetectors rapidly becomes poor due to the obvious degradation of the crystal quality. ZnMgO alloys with a band gap in solar-blind region also suffer from the poor crystal quality due to the phase separation.[9–11]

It is noticed that Ga_2O_3 has a direct wide bandgap of ~4.9 eV, directly corresponding to the wavelength less than 280 nm,[12] is an ideal solar-blind detection material without any doping and alloying process. Among all five phases of Ga_2O_3 (α, β, γ, δ and ε), the β-Ga_2O_3 with monoclinic crystal structure is the thermally and chemically most stable phase, has been widely studied in solar-blind photodetectors.[13–19] So far, β-Ga_2O_3-based photodetectors mainly fall into three categories: film type, single crystals and nanorod arrays (NRAs) type. Compared to thin films, vertical nanowire array structures display more superior optical absorption ability and higher carrier generation, resulting from high surface-to-volume ratio and effective optical coupling, which can further improve the performance of photodetectors.[20–23] He *et al.*[20] first reported the ultraviolet photodetector based on vertical β-Ga_2O_3 nanowire arrays by thermally oxidizing GaN nanowires grown by molecular beam epitaxy (MBE) on Si substrate. Nevertheless, this complexity and high cost in fabrication will limit the practical application of β-Ga_2O_3 NRAs photodetector.

In this work, the vertically aligned β-Ga_2O_3 NRAs are successfully synthesized by economical hydrothermal and simple post-annealed method on fluorine doped tin oxide (FTO) substrate. And then a circular Ti/Au electrode was patterned on β-Ga_2O_3 NRAs to fabricate solar-blind deep ultraviolet photodetectors. The fabricated devices exhibited a great broadband spectral response with the high responsivity

[a]Key Laboratory of Optical Field Manipulation of Zhejiang Province, Center for Optoelectronics Materials and Devices, Department of Physics, Zhejiang Sci-Tech University, Hangzhou, 310018, China. E-mail: dyguo@zstu.edu.cn

[b]Laboratory of Information Functional Materials and Devices, State Key Laboratory of Information Photonics and Optical Communications, School of Science, Beijing University of Posts and Telecommunications, Beijing 100876, China. E-mail: pgli@zstu.edu.cn

[c]College of Materials Science and Engineering, Xiangtan University, Xiangtan 411105, Hunan Province, China

[d]Department of Engineering Materials, University of Sheffield, Mappin Street, Sheffield S1 3JD, UK

[e]China Aerospace Academy of Systems Science and Engineering, Beijing 100876, China

† These authors contributed equally to this work.

exceeding 550 A W^{-1} at −5 V bias voltage. At zero bias, the device shows a photoresponsivity (R_λ) of 10.80 mA W^{-1} and a photo response time of 0.38 s under 254 nm light irradiation with a light intensity of 1.2 mW cm^{-2}, exhibiting a self-powered characteristic. Our findings indicated that this simple synthesize method can be used to fabricate β-Ga_2O_3 NRAs based self-powered solar-blind photodetectors with fast response speed for the potential applications in secure communication and space detection.

2. Experimental details

2.1 Materials

Ethanolamine (C_2H_7NO, 99%), gallium isopropoxide ($C_9H_{21}GaO_3$, 99%), gallium nitrate aqueous solution [$Ga(NO_3)_3 \cdot 9H_2O$, 10%] were purchased from Shanghai Saen Chemical Technology Co., Ltd. Triethanolamine ($C_6H_{15}NO_3$, 78%) was obtained from Hangzhou Gaojing Fine Chemical Industry Co., Ltd. A fluorine doped tin oxide (FTO) with 350 nm conductive layer is used as a substrate. FTO conductive glass (14 Ω cm^{-2}, size: 10 × 20 × 2.2 mm^3) was bought from Japan Nippon Sheet Glass Co., Ltd. All chemicals are analytical grade.

2.2 Synthesis and characterization of the β-Ga_2O_3 NRAs

The GaOOH NRAs were fabricated as described in our previous reports.[24] The substrate coated with Ga_2O_3 seed layer was placed in the growth solution of $Ga(NO_3)_3 \cdot 9H_2O$ and heated at 150 °C for 12 h in an oven. After the growth, the product was washed by DI water, dried in air at 80 °C. The as-prepared GaOOH NRAs calcined at 700 °C for 4 h were converted into the β-Ga_2O_3 NRAs.

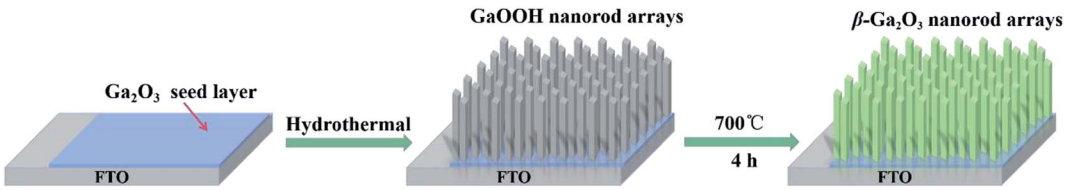

Fig. 1 Schematic illustration of preparation of the β-Ga_2O_3 NRAs.

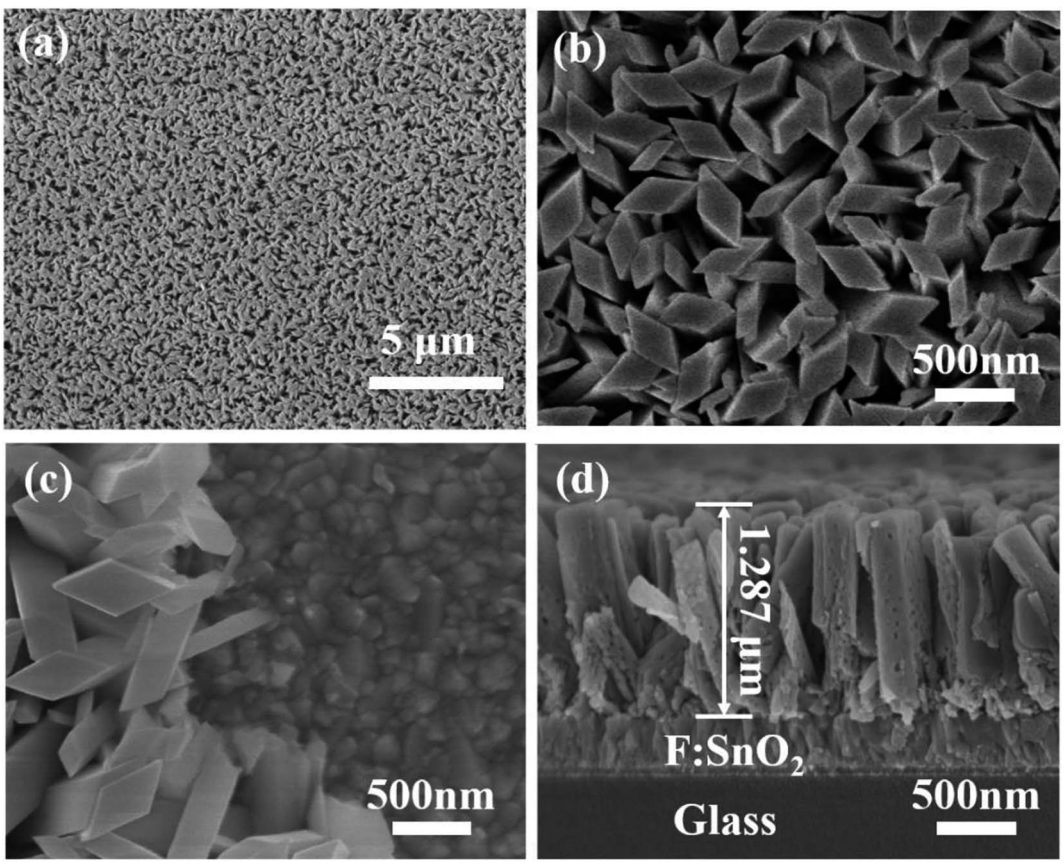

Fig. 2 The top views of SEM images at low (a) and high (b) magnification of β-Ga_2O_3 NRAs grown on the FTO substrate. (c) The edge view of β-Ga_2O_3 NRAs. (d) The cross-section of β-Ga_2O_3 NRAs on the FTO substrate.

The morphologies of β-Ga_2O_3 NRAs were observed by a Hitachi S-4800 field-emission scanning electron microscope (SEM). The crystal structure of samples was analyzed by a Bruker D8 Advance X-ray diffractometer (XRD) using Cu Kα radiation (λ = 0.154 nm). The ultraviolet-visible (UV-vis) absorption spectrum was taken using a Hitachi U-3900 UV-vis spectrophotometer.

2.3 Fabrication and characterization of the photodetector

The photodetector was fabricated by depositing circular Ti/Au electrodes on the vertically aligned β-Ga_2O_3 NRAs with direct current magnetron sputtering. The photoelectric characteristics of the fabricated device were characterized by a Keithley 4200 at room temperature. And a 7 W lamp of 254 nm was used as the UV light source.

3. Results and discussion

The vertically aligned β-Ga_2O_3 NRAs have been grown on the FTO glass substrate and the fabrication process is schematically illustrated in Fig. 1. The β-Ga_2O_3 NRAs is fabricated by three steps procedure: (1) the seed layer was acquired by spin coating ethylene glycol monomethyl ether solution of ethanolamine and gallium isopropoxide onto the FTO substrate; (2) the substrate coated with Ga_2O_3 seed layer was placed in the growth solution of $Ga(NO_3)_3 \cdot 9H_2O$ and heated at 150 °C for 12 h in an oven; (3) the as-prepared GaOOH NRAs calcined at 700 °C for 4 h were converted into the β-Ga_2O_3 NRAs.

The SEM result shows that a large-area, highly dense, and vertically aligned β-Ga_2O_3 NRAs have been successfully grown on the FTO glass substrate [Fig. 2(a–d)]. Fig. 2(a) displays a representative top-view SEM micrograph of as-synthesized β-Ga_2O_3 nanorods. Fig. 2(b) is a magnified image of Fig. 2(a). Fig. 2(c) is a top view SEM image in the boundaries of NRAs. Obviously, there has a high density and flat surface of β-Ga_2O_3 NRAs aligned vertically grown on FTO substrate. It also can be observed that the tips of the nanorods are the diamond shape, whose diameter has changed in the range of 100 to 500 nm. Fig. 2(d) shows the cross-section image of β-Ga_2O_3 NRAs on FTO substrate, we can estimate that the average length of nanorods is ~1.287 μm. Fig. 3(a) shows the XRD patterns of the FTO, FTO/GaOOH and β-Ga_2O_3 NRAs, respectively. In addition to the diffraction peak of the FTO substrate, four peaks located at 35.3°, 37.4°, 62.3° and 66.7° were observed in FTO/GaOOH, which can be indexed to (021), (111), (002) and

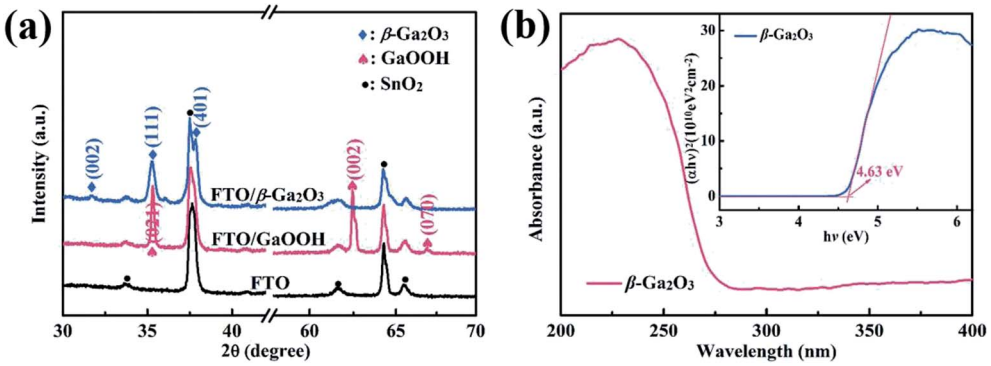

Fig. 3 (a) XRD patterns of the FTO, FTO/GaOOH NRAs and FTO/β-Ga_2O_3 NRAs. (b) The absorption spectrum of β-Ga_2O_3 nanorod, the inset is $(\alpha h\nu)^2$ *versus* $h\nu$.

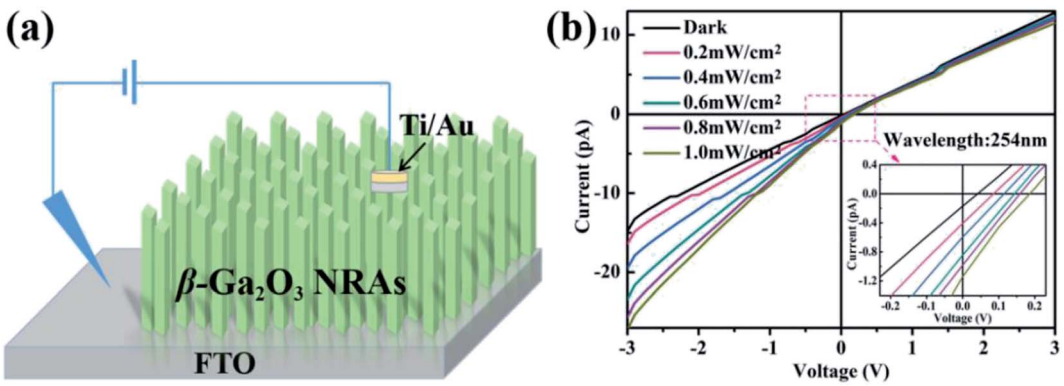

Fig. 4 (a) The schematic diagram of the β-Ga_2O_3 NRAs solar-blind photodetector. (b) *I*–*V* curves of the device in dark and under 254 nm illumination with various light power densities.

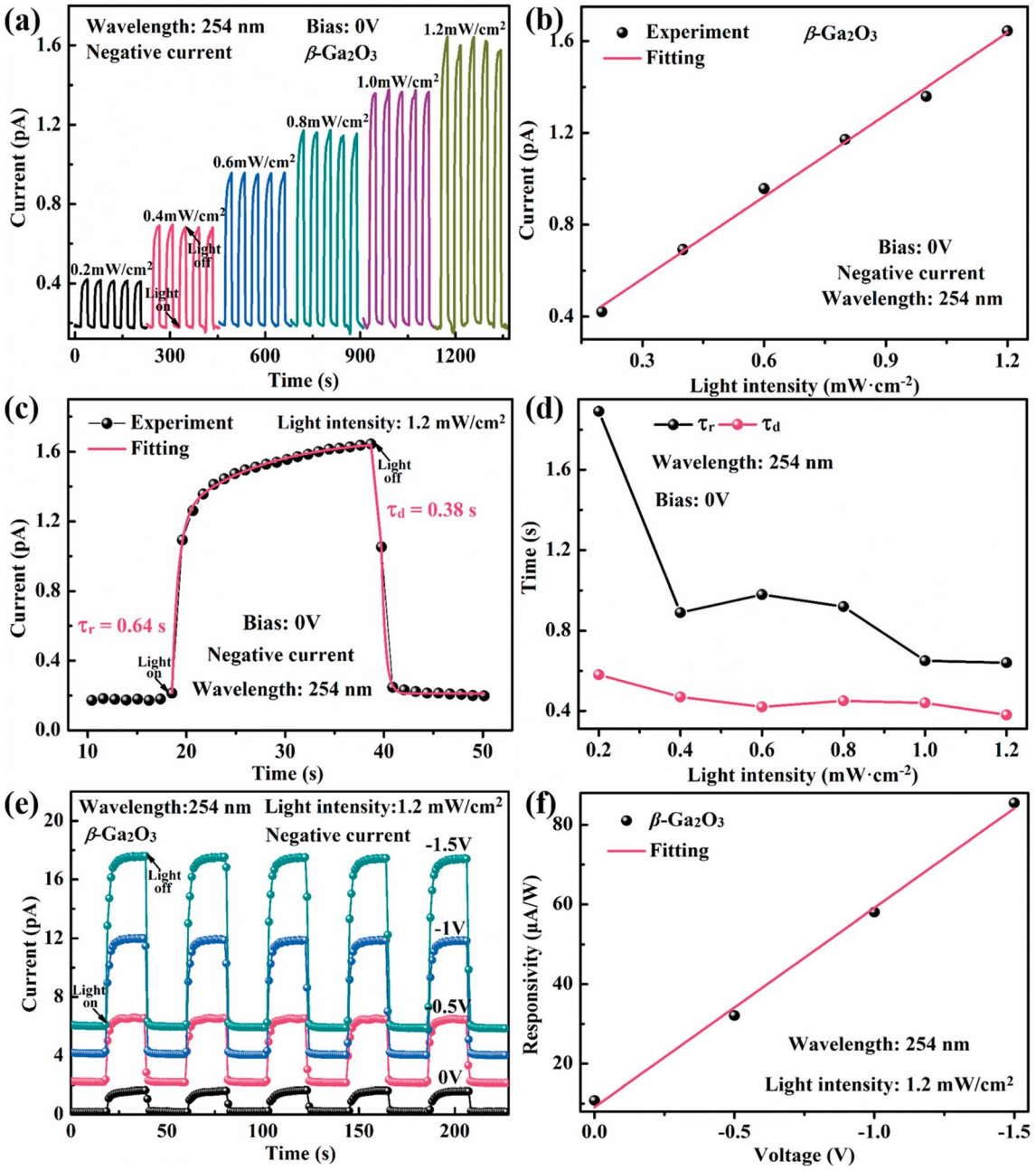

Fig. 5 (a) I–t curves of the device measured at 0 V bias under 254 nm illumination with various light intensities. (b) The relationship between the light intensity and photocurrent. (c) Rise time and decay time of the device at 0 V bias under 254 nm light irradiation with a light intensity of 1.2 mW cm^{-2}. (d) The relationship between the light intensity and photoresponse time. (e) The photoresponse switching behaviors of the device were measured at different applied bias voltages. (f) The relationship between the light intensity and applied bias voltage.

(070) crystal planes of orthorhombic GaOOH (JCPDS file no. 06-0180). The NRAs show a preferred growth orientation of [111] direction. After the annealing of as-prepared GaOOH NRAs, three additional peaks located at 31.7°, 35.3° and 37.9° were observed, which can be ascribed to the (002), (111) and (401) planes of monoclinic β phase of Ga_2O_3 (JCPDS file no. 41-1103).[25] The UV-vis absorbance spectra of the β-Ga_2O_3 NRAs is shown in Fig. 3(b). It shows that the absorption onset of β-Ga_2O_3 is at ~270 nm. The optical bandgaps of β-Ga_2O_3 NRAs can be determined based on the equation: $(\alpha h\nu)^2 = A(h\nu - E_g)$. The energy bandgap ($E_g$) is measured by linear extrapolation to the $h\nu$-axis. The $(\alpha h\nu)^2$ *versus* $h\nu$ curve of the β-Ga_2O_3 NRAs is shown in the inset of Fig. 3(b), the band-gap of β-Ga_2O_3 NRAs was estimated to be ~4.63 eV, which is almost identical with previous reports.[3,20]

A circular Ti/Au electrode was patterned on β-Ga_2O_3 NRAs to fabricate a solar-blind deep ultraviolet photodetector. The schematic diagram of the device is presented in Fig. 4(a). Fig. 4(b) depicts the current voltage (I–V) curves of the device in dark and under 254 nm illumination with various light

Table 1 Comparison of the device parameters of the present β-Ga_2O_3 NRAs based photoresponse parameters and other Ga_2O_3 nanostructures based devices

Materials and structure	UV light	Bias voltage	R (A W^{-1})	EQE (%)	Reference
Ga_2O_3 nanorods	254	0.33	19.31	9427	24
Ga_2O_3 nanowire	255	5	3.43×10^{-3}	1.37	25
GaOOH nanorod	254	0.5	1.07	522	26
Ga_2O_3 nanorods	254	0	1.08×10^{-2}	5.27×10^{-3}	This work

densities. Obviously, under the 254 nm ultraviolet illumination, the current in the reverse bias is larger than that in the forward bias. The inset of Fig. 4(b) is the enlarged curves around zero bias. It can be seen at 0 V bias that the current of the device increases in negative direction with the increase of the light densities, exhibiting a self-powered characteristic.

Fig. 5(a) shows the time-dependent photoresponse (I–t) of the device measured at 0 V bias under 254 nm illumination with various light intensities. It exhibits stable and reproducible characteristics under an on/off interval of 20 s. The dark current is approximately −0.18 pA. Under 254 nm light illumination, along with the light densities increased from 0.2 to 1.2 mW cm^{-2}, the negative photocurrent value of device increase from 0.421 to 1.644 pA. The corresponding light/dark ratios (I_{light}/I_{dark}) are gradually increased from 2.34 to 9.14. Notably, the photocurrent of the device linearly increases with the increase of the light intensities, as shown in Fig. 5(b), revealing that the stronger ultraviolet light can excite more photogenerated carriers. I–t curve of self-powered β-Ga_2O_3 NRAs solar-blind photodetector at 0 V bias under 1.2 mW cm^{-2} 254 nm light irradiation is enlarged in Fig. 5(c). The rising and decaying edges were fitted by an exponential relaxation equation of the following type:

$$I = I_0 + A\,e^{-t/\tau_1} + B\,e^{-t/\tau_2} \quad (1)$$

where I_0 is the steady state photocurrent, t is the time, A and B are constant, τ_1 and τ_2 are two relaxation time constants. τ_r and τ_d are the time constants for the rising edge and fall edge, respectively. The rise time (τ_r) and the decay time (τ_d) of are approximately 0.64 s and 0.38 s respectively.[3] It is noticed in Fig. 5(d) that τ_r and τ_d show downward trend with the increase of light intensity. The photoresponse switching behaviors of the device at different applied bias voltages were measured under 254 nm illumination as shown in Fig. 5(e). Apparently, both the dark current and photocurrent increases along with the increase of the bias voltages ranging from 0 V to −1.5 V. Meanwhile, the photocurrent of 17.60 pA at −1.5 V is about 11 times than that at 0 V under the same conditions. Notably, the photocurrent increases linearly with the increase of the electric field, because a more separation and transportation of electron–hole pairs would excite more pairs of the photo-generated electron–hole, resulting in a higher photocurrent. Photoresponsivity (R_λ) and external quantum efficiency (EQE) are two important parameters to evaluate the sensitivity of PDs. R_λ is defined as the photocurrent generated by per unit power of incident light on the effective area of a PD and EQE is bound up with the number of electron–hole pairs excited by a PD per adsorbed photon and per unit time. R_λ and EQE can be expressed in the following equations:

$$R_\lambda = \Delta I_\lambda / P_\lambda S \quad (2)$$

$$\mathrm{EQE} = hcR_\lambda/(e\lambda) \quad (3)$$

where $\Delta I_\lambda = I_\lambda - I_{dark}$ is the difference between photocurrent and dark current, P_λ is the incident light intensity, S is the effective illuminated area, h is the Planck's constant, c is the velocity of light, e is the electron charge, and λ is the incident light wavelength. It can calculate that the device exhibits a photoresponsivity (R_λ) of 10.80 mA W^{-1} and an external quantum efficiency (EQE) of 5.27×10^{-3}% at 0 V bias under 1.2 mW cm^{-2} 254 nm illumination. Simultaneously, the R_λ and EQE are estimated to 85.52 mA W^{-1} and 4.18×10^{-2}% for −1.5 V bias, respectively. It can be seen from the Fig. 5(f) that R_λ increases near linearly with the bias voltage. Accordingly, applying bias voltage is a good way to rationally optimize the photoelectric performance of photodetector. For comparison, we list the photoresponse parameters of β-Ga_2O_3 NRAs PD and other types of devices reported in the literature in Table 1. It can be seen that compared with the other type device our device can work at zero bias. The β-Ga_2O_3 NRAs PD with a simple structure renders relatively high performance, wide absorption region and low fabrication cost, promising building high performance optoelectronic devices with a self-powered worked characteristic in the future.

4. Conclusions

In conclusion, a self-powered solar-blind photodetector was successfully fabricated by simple and low cost β-Ga_2O_3 NRAs growth process. The fabricated β-Ga_2O_3 NRAs based PD showed an obvious photoresponse in solar-blind ultraviolet region with good repeatability and stability. Under 0 V bias and 1.2 mW cm^{-2} 254 nm illumination, the photodetector exhibits a I_{light}/I_{dark} ratio of 9.14, a R_λ of 10.80 mA W^{-1}, τ_r of 0.64 s and τ_d of 0.38 s. The self-powered photodetector based on β-Ga_2O_3 NRAs with high light-to-electron conversion and low power consumption abilities is a promising candidate for solar-blind photodetection application.

Conflicts of interest

There are no conflicts to declare.

Acknowledgements

This work was supported by the National Natural Science Foundation of China (No. 61704153, 51572241, 61774019, 51572033, 11605149), Zhejiang Public Service Technology Research Program/Analytical Test (LGC19F040001), Open Fund of IPOC (BUPT), and Science and Technology Department of Zhejiang Province Foundation (2017C37017).

References

1 L. W. Sang, M. Y. Liao, M. Sumiya, *et al.*, A comprehensive review of semiconductor ultraviolet photodetectors: from thin film to one-dimensional nanostructures, *Sensors*, 2013, **13**(8), 10482–10518.

2 D. S. Tsai, W. C. Lien, D. H. Lien, *et al.*, Solar-blind photodetectors for harsh electronics, *Sci. Rep.*, 2013, **4**(9), 2628.

3 B. Zhao, F. Wang, H. Y. Chen, *et al.*, Solar-blind avalanche photodetector based on single ZnO–Ga_2O_3 core–shell microwire, *Nano Lett.*, 2015, **15**(6), 3988.

4 Q. Zhang, J. S. Jie, S. L. Diao, *et al.*, Solution-processed graphene quantum dot deep-UV photodetectors, *ACS Nano*, 2015, **9**(2), 1561–1570.

5 N. Shouleh, H. Michael, D. J. April, *et al.*, Single photon counting UV solar-blind detectors using silicon and III-nitride materials, *Sensors*, 2016, **16**(6), 927.

6 C. Y. Cho, Y. Zhang, E. Cicek, *et al.*, Surface plasmon enhanced light emission from AlGaN-based ultraviolet light-emitting diodes grown on Si (111), *Appl. Phys. Lett.*, 2013, **102**, 211110.

7 F. H. Teherani, D. C. Look, D. J. Rogers, *et al.*, Optical properties of ZnMgO films grown by spray pyrolysis and their application to UV photodetection, *Semicond. Sci. Technol.*, 2015, **30**(10), 105026.

8 X. C. Guo, N. H. Hao, D. Y. Guo, *et al.*, β-Ga_2O_3/p-Si heterojunction solar-blind ultraviolet photodetector with enhanced photoelectric responsivity, *J. Alloys Compd.*, 2016, **660**, 136–140.

9 K. W. Liu, M. Sakurai and M. Aono, ZnO-based ultraviolet photodetectors, *Sensors*, 2010, **10**, 8604–8634.

10 L. K. Wang, Z. G. Ju, J. Y. Zhang, *et al.*, Single-crystalline cubic MgZnO films and their application in deep-ultraviolet optoelectronic devices, *Appl. Phys. Lett.*, 2009, **95**, 131113.

11 X. L. Du, Z. X. Mei, Z. L. Liu, *et al.*, Controlled growth of high-quality ZnO-based films and fabrication of visible-blind and solar-blind ultra-violet detectors, *Adv. Mater.*, 2009, **21**, 4625–4630.

12 Y. P. Qian, D. Y. Guo, X. L. Chu, *et al.*, Mg-doped p-type β-Ga_2O_3 thin film for solar-blind ultraviolet photodetector, *Mater. Lett.*, 2017, **209**, 558–561.

13 D. Y. Guo, X. L. Zhao, Y. S. Zhi, *et al.*, Epitaxial growth and solar-blind photoelectric properties of corundum-structured α-Ga_2O_3 thin films, *Mater. Lett.*, 2016, **164**, 364–367.

14 D. Y. Guo, Y. L. Su, H. Z. Shi, *et al.*, Self-powered ultraviolet photodetector with super high photoresponsivity (3.05 A/W) based on the GaN/Sn:Ga_2O_3 pn junction, *ACS Nano*, 2018, **12**, 12827–12835.

15 D. Y. Guo, H. Liu, P. G. Li, *et al.*, Zero-power-consumption solar-blind photodetector based on β-Ga_2O_3/NSTO heterojunction, *ACS Appl. Mater. Interfaces*, 2017, **9**(2), 1619–1628.

16 D. Y. Guo, H. Z. Shi, Y. P. Qian, *et al.*, Fabrication of β-Ga_2O_3/ZnO heterojunction for solar-blind deep ultraviolet photodetection, *Semicond. Sci. Technol.*, 2017, **32**(3), 03LT01.

17 D. Y. Guo, Z. P. Wu, P. G. Li, *et al.*, Fabrication of β-Ga_2O_3 thin films and solar-blind photodetectors by laser MBE technology, *Opt. Mater. Express*, 2014, **4**(5), 1067.

18 L. P. Dong, R. X. Jia, C. Li, *et al.*, Ab initio study of N-doped β-Ga_2O_3 with intrinsic defects: the structural, electronic and optical properties, *J. Alloys Compd.*, 2017, **712**, 379–385.

19 H. P. Zhang, R. X. Jia, L. Yuan, *et al.*, Leakage current conduction mechanisms and electrical properties of atomic-layer-deposited HfO_2/Ga_2O_3 MOS capacitors, *J. Phys. D: Appl. Phys.*, 2018, **51**(7), 1.

20 T. He, Y. K. Zhao and X. D. Zhang, Solar-blind ultraviolet photodetector based on graphene/vertical Ga_2O_3 nanowire array heterojunction, *Nanophotonics*, 2018, **7**, 1557.

21 H. O. Li, Y. Li, G. L. Xiao, *et al.*, Simple fabrication ZnO/β-Ga_2O_3 core/shell nanorod arrays and their photoresponse properties, *Opt. Mater. Express*, 2018, **8**, 794.

22 W. W. Zhong, S. J. Shen, S. S. Feng, *et al.*, Facile fabrication of alveolate $Cu_{2-x}Se$ microsheets as a new visible-light photocatalyst for discoloration of Rhodamine B, *CrystEngComm*, 2018, **20**, 7851.

23 W. W. Zhong, W. G. Tu, S. S. Feng, *et al.*, Photocatalytic H_2 evolution on CdS nanoparticles by loading FeSe nanorods as co-catalyst under visible light irradiation, *J. Alloys Compd.*, 2019, **772**, 669–674.

24 Y. L. Wu, S. J. Chang, W. Y. Weng, *et al.*, Ga_2O_3 nanowire photodetector prepared on SiO_2/Si template, *IEEE Sens. J.*, 2013, **13**, 2368–2373.

25 H. J. Lin, J. P. Baltrus, H. Y. Gao, *et al.*, Perovskite nanoparticle-sensitized Ga_2O_3 nanorod arrays for CO detection at high temperature, *ACS Appl. Mater. Interfaces*, 2016, **8**, 8880.

26 K. Chen, C. R. He, D. Y. Guo, *et al.*, Low-voltage-worked photodetector based on Cu_2O/GaOOH shell-core heterojunction nanorod arrays, *J. Alloys Compd.*, 2018, **755**, 199–205.